Field-induced forces in colloidal particle chains

H. Zhang and M. Widom
Department of Physics, Carnegie-Mellon University, Pittsburgh, Pennsylvania 15213
(Received 21 October 1994)

Electrorheological and magnetorheological effects occur when applied fields polarize particles dissolved in solution. When dipole interaction energies between particles are comparable to thermal energies and particle volume fraction is low, particles align in chains. This paper considers the dipole and higher moment forces within such a chain. We examine forces due to interactions beyond nearest neighbors within a chain, mutual polarization of the particles, and distortion of particle shapes by the applied field. Thermal expansion of the chain enters in the limit of weak applied field.

PACS number(s): 64.70.Dv, 05.20.−y, 64.70.Rh

I. INTRODUCTION

Electrorheological and magnetorheological fluids are colloidal suspensions of particles in a solvent where particle and solvent polarizabilities differ. Electrorheological fluids, for example, may consist of cornstarch and water particles dissolved in oil. These particles have a high electrical polarizability compared with oil. In the presence of a strong external electric field the polarizable particle adds a dipole moment to the electric field in its vicinity. Dipole moments tend to line up in chains or columns, altering the fluid's viscosity [1].

An interesting magnetic analog of such a system is ferrofluid emulsion [2,3], a suspension of oil based ferrofluid droplets in water (Fig. 1). The size of the droplets ranges from a fraction of a micrometer to a few micrometers. Sodium dodecyl sulfate (SDS) surfactant molecules on the droplet surface reduce the surface tension between the water and oil components. Through a process of fractionation, the emulsion can be made highly monodisperse.

Like ferrofluids, a ferrofluid emulsion appears brown.

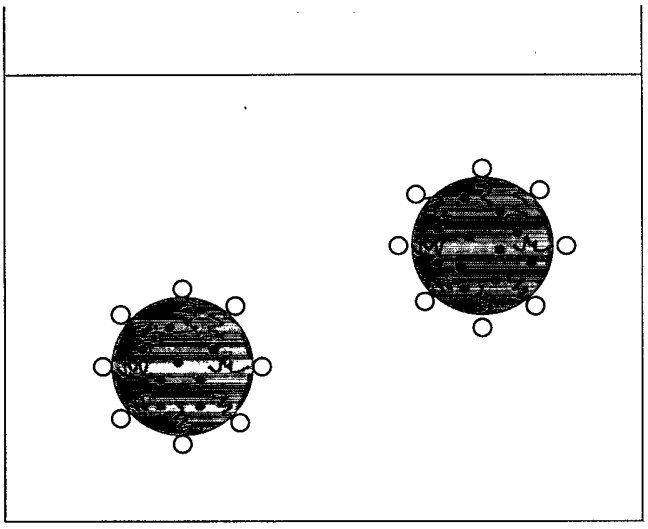

FIG. 1. Schematic representation of a ferrofluid emulsion. Amphiphilic molecules separate oil-based ferrofluid from water.

However, when illuminating a monodisperse ferrofluid emulsion with white light parallel to the applied field, the backscattering displays beautiful colors such as red, yellow, green, or blue, depending on the applied field strength [2,3]. This phenomenon results from chain formation in the field direction. For a perfectly aligned chain with particle spacing d, the first-order backscattering peaks at wavelength

$$\lambda_0 = 2nd \ , \tag{1}$$

where n is the refractive index of the suspending medium ($n = 1.33$ for water).

Field-induced droplet chains offer a technique for direct measurements of the force-distance laws between colloidal liquid droplets [2]. Such measurements have been an outstanding challenge since colloidal forces are extremely weak ($\sim 10^{-13}$–10^{-11} N) and colloidal separation is difficult to control with accuracy. As a result, the force-distance laws have hitherto been primarily inferred from bulk properties and phase behavior. Introducing a magnetic ingredient, however, enabled Bibette and coworkers [2,3] to measure both force and distance precisely. An applied field causes droplets to form chains in the field direction, so they can infer droplet separation from the backscattering peak wavelength using Eq. (1).

This paper calculates the magnetic attraction induced by applied fields in terms of the sphere diameter and ferrofluid susceptibility. The experimental study [2] uses our calculation of magnetic attraction as well as Hamaker's [4] estimate of van der Waals attraction to obtain the net attractive force. The remaining colloidal forces must exactly balance the magnetic and van der Waals attractions. The repulsive forces thus measured show excellent agreement with established theories on screened Coulomb repulsion in ionic colloidal systems.

The experiments [2] are performed on dilute emulsions, where chains are well defined, droplets are well spaced, and backscattering peaks are distinct, making theoretical predictions of force laws relatively simple. The droplet volume fraction $\phi < 0.1\%$, and droplet radius $r_0 = 94$ nm. For the magnetic field $\sim 10^4$ A/m used in the experiment, the ferrofluid in the droplets remains homogeneous, and the droplets remain almost perfectly spherical. Chains are one droplet thick and about 30 droplets long,

and are well separated from each other.

This paper has two main technical sections. Section II calculates the forces between droplets resulting from dipole moments. We show that mutual induction of droplets, and long-range interactions between droplets within a chain, dramatically influence the net magnetic force. Section III estimates other contributions to the force from quadrupole and higher magnetic moments. Such higher moments can arise from nonuniformity of local magnetic fields in the vicinity of each droplet, or from droplet deformation. We show that deformation may be ignored, but nonuniformity of the field is important when the droplets are nearly in contact. Finally, we summarize our results and mention the importance of thermal expansion in the weak field limit.

II. DIPOLE FORCE

We study the magnetic forces acting within a field-induced droplet chain as a function of applied field $\mathbf{H}_0$ and droplet separation d. The dominant force is the dipole-dipole interaction. For two dipoles $\mathbf{m}_1=\mathbf{m}_2=\mathbf{m}$ parallel to their separation $\mathbf{d}$, their attractive force is

$$F_{\text{pair}}=-\frac{6m_1m_2}{d^4}=-\frac{6m^2}{d^4}\ . \tag{2}$$

In calculating the induced dipole moment m of each droplet, we must include dipole fields from other droplets in addition to the applied field. In calculating the dipole force within a chain, we must sum up the interaction over all particles. In addition to the dipole moment, each droplet possesses quadrupole and higher moments resulting from the field gradient and aspherical shape (see Fig. 2).

For weak fields the magnetization $\mathbf{M}$ in a droplet is linear in external field $\mathbf{H}_{\text{ext}}$ with a shape dependent coefficient χ_{shape},

$$\mathbf{M}=\chi_{\text{shape}}\mathbf{H}_{\text{ext}}=\frac{\chi}{1+4\pi N\chi}\mathbf{H}_{\text{ext}}\ , \tag{3}$$

where χ is the shape independent intrinsic susceptibility related to relative permeability $\mu=1+4\pi\chi$, and N is the shape dependent demagnetization factor. The shape independent intrinsic susceptibility $\chi=0.18$ measured from the bulk ferrofluid. For a sphere, $N=\frac{1}{3}$, so the shape dependent susceptibility is $\chi_{\text{sphere}}\approx 0.10$. A droplet with radius r_0 has a magnetic moment

$$\mathbf{m}=\mathbf{M}V=\frac{4\pi}{3}r_0^3\chi_{\text{sphere}}\mathbf{H}_{\text{ext}}\ . \tag{4}$$

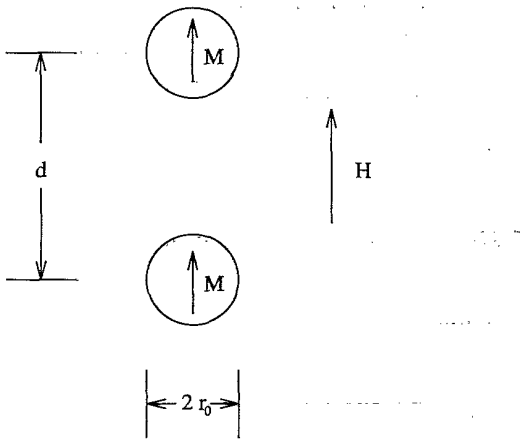

FIG. 2. Field and magnetization geometry for two interacting droplets.

A. Mutual induction

When two dipole moments align with separation $\mathbf{d}$ parallel to the field direction, each generates a field at the center of the other:

$$\mathbf{H}_1=\frac{2\mathbf{m}}{d^3}\ . \tag{5}$$

Now the external field $\mathbf{H}_{\text{ext}}$ acting on the droplet is the sum of applied field $\mathbf{H}_0$ and dipole field $\mathbf{H}_1$,

$$\mathbf{H}_{\text{ext}}=\mathbf{H}_0+\mathbf{H}_1\ . \tag{6}$$

Combining Eq. (4) for $\mathbf{m}$ in terms of $\mathbf{H}_{\text{ext}}$ with Eqs. (5) and (6) for $\mathbf{H}_{\text{ext}}$ in terms of $\mathbf{H}_0$ and $\mathbf{m}$ gives the magnetic moment in terms of applied field:

$$\mathbf{m}=\frac{\frac{4\pi}{3}r_0^3\chi_{\text{sphere}}}{1-\frac{8\pi}{3}\left[\frac{r_0}{d}\right]^3\chi_{\text{sphere}}}\mathbf{H}_0\ . \tag{7}$$

Noting that $\chi_{\text{sphere}}\approx 0.10$ for the experimental sample, Eq. (7) shows that mutual induction increases the droplet magnetic moment by about 12% if the two droplets are in contact ($d=2r_0$), and by a smaller amount if they are separated. Putting this magnetic moment into Eq. (2) for the dipole force increases the pair dipole attraction F_{pair} by up to 25%.

B. Chaining effects

For a particle within an infinitely long chain of particles with equal spacing d, the total dipole field from all other particles is

$$\mathbf{H}_1=2\sum_{n=1}^{\infty}\frac{2\mathbf{m}}{(nd)^3}=4\zeta(3)\frac{\mathbf{m}}{d^3}\ , \tag{8}$$

where $\zeta(3)=\sum_{n=1}^{\infty}1/n^3=1.202$ is the Riemann ζ function. Equivalent results for chains and three-dimensional crystals have been calculated for electrorheological fluids [5,6]. Finite chain length may reduce the ζ function. For the chain lengths in the ferrofluid emulsion, the ζ function is accurate to within 0.1:

$$\mathbf{m}=\frac{\frac{4\pi}{3}r_0^3\chi_{\text{sphere}}}{1-\frac{16\pi\zeta(3)}{3}\left[\frac{r_0}{d}\right]^3\chi_{\text{sphere}}}\mathbf{H}_0\ . \tag{9}$$

Consider an infinite chain consisting of droplets connected head to tail with $d=2r_0$. For a given applied field $\mathbf{H}_0$,

a droplet in an infinite chain is about 34% more magnetized (taking $\chi_{\text{sphere}} \approx 0.10$) than in isolated droplet.

To calculate the attractive dipole force within an infinitely long chain, we choose an arbitrary point between any two adjacent particles and note that n bonds of length nd span the point. The total attractive force of all these bonds is thus

$$F_{\text{chain}} = -\sum_{n=1}^{\infty} n\frac{6m^2}{(nd)^4} = -\zeta(3)\frac{6m^2}{d^4} . \tag{10}$$

Comparing Eq. (10) for F_{chain} and Eq. (2) for F_{pair}, we note that, for the same magnetic moment m, F_{chain} is 20% stronger than F_{pair}. We already showed [Eq. (9)] that for the same applied field strength H_0, the magnetic moment of a particle in a long chain exceeds that of an isolated particle by 34%. Compounding the two effects, the actual force within a chain can exceed the force naively calculated from Eqs. (2) and (4) by a factor as large as $1.20 \times 1.34^2 = 2.15$.

III. HIGHER MOMENTS

The magnetic force between the droplets depends on their magnetic multipole moments. Dipole-dipole interaction only contributes the leading term. Higher moments arise from two sources. First applied field elongates a deformable particle. Second, the dipole field of one particle on another varies by $\sim 12mr_0/d^4$ across the particle of radius r_0. This spatially varying field induces nonuniform magnetization.

A. Elongation

An unmagnetized droplet has a spherical shape which minimizes surface energy. A uniformly magnetized droplet elongates parallel to the magnetization to lower the magnetic energy. For strong surface tension σ, such elongation is very small, and we can approximate the droplet shape with a prolate spheroid with eccentricity $e \ll 1$. Its radius at polar angle θ relative to the rotationally symmetric axis (length $2a$) is

$$r(\theta) = \frac{b}{(1-e^2\cos^2\theta)^{1/2}} , \tag{11}$$

where $2b$ is the degenerate minor axis, and

$$b = r_0(1-e^2)^{1/6} , \tag{12}$$

under the fixed volume constraint $[V = (4\pi/3)r_0^3]$ for an incompressible fluid.

We can study magnetic moments using the effective magnetic charge picture. In a uniformly magnetized medium, bulk magnetic charge density $\rho_M = -\nabla\cdot\mathbf{M} = 0$. In other words, the droplet have only surface charge density

$$\sigma_m = \mathbf{n}\cdot\mathbf{M} , \tag{13}$$

where $\mathbf{n}$ is the unit normal vector pointing outwards. We write the magnetic multipole moments caused by surface charge density σ_m in spherical coordinates,

$$q_{lm} = \int Y_{lm}^*(\theta,\phi) r^l \sigma_m dS , \tag{14}$$

where r is the distance between the point on the surface to the droplet center. Multipole moments in spherical coordinates and in Cartesian coordinates have simple relations. For example, dipole moment $m = \sqrt{4\pi/3}q_{10}$, quadrupole moment $Q_{zz} = 2\sqrt{4\pi/5}q_{20}$, and so on.

All $m \neq 0$ moments vanish due to rotational symmetry about the direction of magnetization $\mathbf{M}$. For $m = 0$, the spherical harmonic $Y_{l0}^*(\theta,\phi)$ is simply the Legendre function $P_l(\cos\theta)$ multiplied by a constant

$$Y_{l0}^*(\theta,\phi) = \left[\frac{2l+1}{4\pi}\right]^{1/2} P_l(\cos\theta) . \tag{15}$$

Letting $z = \cos\theta$, the surface integral for the nonvanishing moments in Eq. (14),

$$A_l \equiv q_{l0} = \sqrt{(2l+1)\pi}\int_{-1}^{1} P_l(z) r^{l+2}(z)\sigma_m(z)dz . \tag{16}$$

Surface magnetic charge density depends on droplet shape:

$$\sigma_m(z) = M\frac{zr(z) - (1-z^2)r'(z)}{\sqrt{r(z)^2 + (1-z^2)r'(z)^2}} = M\frac{(1-e^2)z}{\sqrt{1-2e^2z^2+e^4z^2}} . \tag{17}$$

For a uniformly magnetized droplet, $f(z)$ is even in z and $\sigma_m(z)$ is odd. Therefore,

$$A_{l=\text{even}} = 0 . \tag{18}$$

In other words, since uniform magnetization corresponds to $l = 1 = \text{odd}$, it only generates moments with odd l. To estimate the nonvanishing moments, note that if we expand $r(z)^{l+2}\sigma_m(z)$ in powers of z, the z^l term is of order e^{l-1}. Thus orthogonality of Legendre polynomials yields

$$A_{l=\text{odd}} \sim Mr_0^{l+2}e^{l-1} . \tag{19}$$

For a uniformly magnetized droplet, the quadrupole moment vanishes, the octupole moment is of order e^2, and so on.

Competition between magnetic and surface energies determines the eccentricity e. For a slightly prolate ellipsoid, the demagnetization factor

$$N = \tfrac{1}{3} - \tfrac{2}{15}e^2 + \mathcal{O}(e^4) . \tag{20}$$

By reducing N, elongation lowers demagnetization energy,

$$\Delta E_{\text{dem}} = -\tfrac{1}{2}\times 4\pi(N-\tfrac{1}{3})M^2V \approx -\frac{16\pi^2}{45}e^2M^2r_0^3 , \tag{21}$$

to leading order in eccentricity e. On the other hand, elongation increases the surface area. Using Eqs. (11) and (12) for the shape of a spheroid, we obtain the surface energy change

$$\Delta E_{\text{sur}} = \sigma\Delta S \approx \frac{8\pi}{45}e^4r_0^2\sigma \tag{22}$$

to leading order in eccentricity e. σ is the surface tension

and ΔS is the increase in surface area. Consequently total energy minimization yields the equilibrium eccentricity

$$e^2=\pi\frac{r_0}{\sigma}M^2 . \tag{23}$$

Droplet radius $r_0\approx 10^{-5}$ cm and surface density $\sigma\approx 15$ dyn/cm^2. For a typical applied field strength $H_0\sim 2\times 10^4$ A/m$\sim$250 Oe and $\chi_{\text{sphere}}\approx 0.10$, magnetization $M\sim 25$ emu/cm^3. Equation (23) yields eccentricity

$$e^2\sim 1.3\times 10^{-3} . \tag{24}$$

Consequently, the major axis $a\sim(1+4\times 10^{-4})r_0$ and minor axis $b\sim(1-2\times 10^{-4})r_0$. The elongation is slight, as observed in experiments. Since $A_3\sim e^2$, the resulting octupole moment can be neglected in comparison with the dipole.

It is interesting to contrast this result with a calculation of elongation in electrorheological fluids by Halsey and Toor [1]. Phase separation of dense electrorheological fluid droplets is induced by application of an electric field to a dilute suspension. The electric field drives the phase separation, and hence creates the surface tension. Depolarization forces and surface tension both vary as the square of applied field, so the droplets possess a field independent elongation, which may be quite substantial for large droplets.

B. Field gradients

If we put two droplets nearby in a uniform applied field, their magnetization becomes nonuniform, and they acquire multipole moments from mutual induction even if they have spherical shape. Even though $\mathbf{M}$ becomes nonuniform, the bulk magnetic charge density $\rho_M\equiv\nabla\cdot\mathbf{M}=0$, provided the ferrofluid uniformly fills the droplet, since in that case we have $\mathbf{M}\sim\mathbf{B}$ and, of course, $\nabla\cdot\mathbf{B}=0$. We therefore only need to study the surface charge [see Eq. (16)].

Recall relation (16) of the moments A_l to surface charge density σ_m, and relation (13) of surface charge density to magnetization $\mathbf{M}$. Assume the nonuniform magnetization in one sphere is induced by the dipole moment $\mathbf{m}$ in a nearby sphere a distance d away, so $\mathbf{M}=\chi\mathbf{H}_{\mathbf{m}}$ with $\mathbf{H}_{\mathbf{m}}$ the dipole field. We expand the resulting surface charge density in Legendre polynomials (see Fig. 3):

$$\sigma_m(\cos\theta)=\frac{\chi^m}{d^3}\sum_{l=1}^{\infty}(-1)^{l+1}l(l+1)\left[\frac{r_0}{d}\right]^{l-1}P_l(\cos\theta) . \tag{25}$$

Integrating over the surface in Eq. (16) yields the multipole moments A_l. Meanwhile, we evaluate the force between dipole moment m and multipole moment A_l:

$$F_{D-l}=(-1)^l(l+1)(l+2)\left[\frac{4\pi}{2l+1}\right]^{1/2}\frac{mA_l}{d^{l+3}} . \tag{26}$$

This result incorporates the dipole-dipole force (2) as a special case.

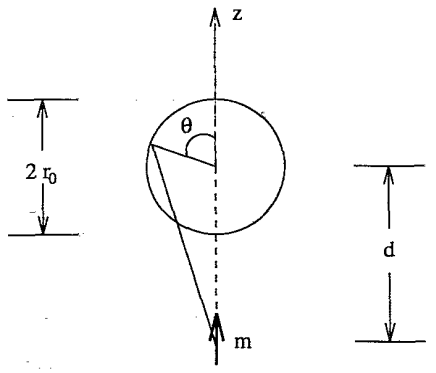

FIG. 3. Geometry for expansion of surface charge σ_m due to external dipole moment $\mathbf{m}$.

Comparing the force F_{D-l} between dipole m and induced multipole moment A_l with the dipole-dipole force F_{D-D} [given by Eq. (2)],

$$\frac{F_{D-l}}{F_{D-D}}=\frac{2\pi}{3}\chi\left[\frac{l(l+1)^2(l+2)}{2l+1}\right]\left[\frac{r_0}{d}\right]^{2l+1} . \tag{27}$$

Although these interactions fall off faster than the dipole-dipole interaction at large separation d, for small $d=2r_0$ and large susceptibility $\chi=0.18$ they can be quite large. For example, the quadrupole moment ($l=2$) contributes $F_{D-Q}=0.17F_{D-D}$, and adding up interactions of all moments $l\geq 2$ yields

$$\sum_{l=2}^{\infty}F_{D-l}=0.35F_{D-D} , \tag{28}$$

when $d=2r_0$, but becomes less important as d increases.

In an infinite chain all even multipole moments vanish due to antisymmetry of the magnetization under spatial inversion through the center of any droplet. The factor of 0.35 in Eq. (28) falls to 0.126 when the sum starts at the octupole moment ($l=3$). But incorporating the factor of 2 into the strength of the odd multipoles due to interactions with two neighboring droplets raises the contribution back to $0.25F_{D-D}$.

We can also look at interactions of higher moment droplets further down the chain. The dipole-octupole interaction picks up $\zeta(5)=1.037$, and higher moments acquire ζ functions of even larger arguments. These interactions are entirely negligible. What about the interaction of higher moments with each other? These forces contains an extra factor of susceptibility χ so they never exceed a few percent of the total.

IV. CONCLUSIONS

This paper studies magnetic forces between droplets magnetized by a uniform applied field $\mathbf{H}_0$. We discuss forces both between 2 droplets and within a long chain. The dominant force is the dipole-dipole force. Mutual induction of droplets within a chain enhances their magnetization by up to 34% beyond the magnetization of an identical droplet in isolation. Since the dipole interaction

is long ranged, neighbors other than the nearest contribute significantly to both mutual induction and dipole-dipole attraction within a long chain. This mechanism adds to the forces within a chain by more than 20%. Together these effects generate a correction of over a factor of 2 to the most naive calculation of forces. Higher moments due to nonuniformity of the dipole field fall off more rapidly than the dipole interaction at large separation. However, at small separation these forces amount to 25% of the dipole-dipole force F_{pair} given by Eq. (2). All together, these corrections amount to a factor $(1+0.20+0.25)\times 1.34^2=2.60$.

Our study addresses only the weak field regime where magnetization is linear in field strength. When saturation sets in, our treatment of demagnetization and mutual induction is no longer appropriate, and we must modify our calculation of magnetization. In the case of full saturation, for example, we simply set $M=M_s$, where M_s is the saturation magnetization. Once we obtain the dipole moment, we use the same formula to calculate the dipole-dipole force. Saturation also homogenizes magnetization in the droplets and thus diminishes higher moments caused by mutual induction.

In the limit of very weak fields the magnetic interaction energies become comparable to thermal energies. In this case, thermal equilibrium spacings $d(T)$ are determined statistically, and differ from the mechanical equilibrium spacing d_0 determined by a balance of forces. It is well known [7] that nonlinearities in force vs separation laws generate thermal expansion:

$$\Delta d \equiv d(T)-d_0 \approx \frac{F_2}{2F_1^2} k_B T \ , \tag{29}$$

where F_n denotes the nth derivative of total force $F=F^e+F^m$ at the point of equilibrium where the total force vanishes. In our case the important contributions to F are the magnetic attraction $F^m=-6(\chi H)^2/d^4$ and the electrostatic repulsion F^e dominated, for large ionic strength, by exponential screening $e^{-\kappa d}$. Hence the derivatives $F_1^e \approx \kappa F^e$ and $F_2^e \approx \kappa^2 F_e$. In contrast, derivatives of the magnetic force fall off as powers of d. So $|F_n^e| \gg |F_n^m|$, provided we have strong screening $\kappa d \gg 1$. The thermal expansion becomes simply

$$\Delta d \approx \frac{k_B T}{2F^e} \ . \tag{30}$$

Consequently the thermal equilibrium value of $d(T)$ is greater than the d_0 predicted by a simple balance of forces. The discrepancy is greatest in weak magnetic fields, since then $F^e=-F^m$ is small. Taking $k_B T=4\times 10^{-21}$ J and force $F^e \approx 10^{-12}$ N as in Bibette's experiment yields a small but possibly measurable deviation $\Delta d \approx 2$ nm. This may explain the small deviation of the force vs distance law from the theoretical predictions observed in strongly ionic emulsions at weak fields [2]. Alteratively, those deviations may be due to higher moment interactions which fall off quickly at large separation.

Our results can also be applied to electrorheological fluids, the electric counterpart of magnetic fluids. However, interactions with electrodes play a significant role in electrorheological fluids [1,5], but have not been included in the present analysis. We may also consider electric and magnetic holes in which the solvent polarizability is greater than the particles. In this case the induced dipole moments point opposite to the applied external fields. When applying our results to any such systems, all we need to do is replace intrinsic susceptibility χ with intrinsic susceptibility different $\chi_{\text{drop}}-\chi_{\text{carrier}}$, where χ_{drop} and χ_{carrier} are the intrinsic susceptibilities of the droplet fluid and the carrier fluid, respectively. Of course, detailed conclusions about the relative importance of forces considered in this study apply only to the specific ferrofluid emulsion considered in Refs. [2] and [3].

ACKNOWLEDGMENTS

We thank J. Bibette for motivating this work and for fruitful discussions. This work was supported in part by NSF Grant No. DMR-9221596.

[1] T. C. Halsey and W. Toor, Phys. Rev. Lett. **65**, 2820 (1990).
[2] F. L.Calderon, T. Stora, O. M. Monval, P. Poulin, and J. Bibette, Phys. Rev. Lett. **72**, 2959 (1994).
[3] J. Bibette, J. Magn. Magn. Mater. **122**, 37 (1993).
[4] H. C. Hamaker, Physica **4**, 1058 (1937).
[5] W. Toor and T. C. Halsey, Phys. Rev. A **45**, 8617 (1992).
[6] R. Tao and J. M. Sun, Phys. Rev. Lett. **67**, 398 (1991).
[7] C. Kittel, *Introduction to Solid State Physics,* 6th ed. (Wiley, New York, 1986), p. 115.